



Lightning Induced Overvoltages on Overhead Lines Shielded by Nearby Buildings

F. Tossani, A. Borghetti, F. Napolitano, C.A. Nucci
Dept. of Electrical, Electronic and Information Engineering
University of Bologna
Bologna, Italy

A. Piantini
Institute of Energy and Environment
University of Sao Paulo
Sao Paulo, Brazil

Abstract— In urban areas the presence of buildings is expected to reduce the amplitude of lightning induced voltages on overhead lines with respect to the case of open terrain. This paper presents a method for estimating such a reduction effect. For this purpose weighting functions are applied to the electrostatic, induction and radiation terms of the expressions adopted for the lightning electromagnetic field calculation assuming open terrain. The parameters of the weighting functions are identified by means of a least square fitting procedure using a finite element method model as benchmark for the field calculation. These functions are shown to be rather independent of the lightning return stroke current waveform and of the distance between the line and the stroke location. Although this paper presents only results obtained for the case of a single line, the method is conceived in order to be applicable for the lightning performance assessment of more complex power distribution networks.

Keywords—finite element method, lightning-induced voltage, shielding effect of nearby buildings.

I. INTRODUCTION

The evaluation of the lightning performance of power distribution networks located in urban areas is complicated by the presence of buildings. The effect of close-by buildings may reduce the lightning electromagnetic pulse (LEMP), as experimentally observed and discussed in [1] and references therein, and represents indeed one of the factors that adds up to the problem complexity. The appraisal of lightning induced overvoltages on overhead lines partially shielded by nearby buildings has been recently addressed by using reduced scale models [2], [3], of three dimensional (3D) finite-difference time-domain (FDTD) models [4], and of finite element method (FEM) models [5].

In [5] the FEM model is used for the calculation of the lightning electromagnetic pulse (LEMP), whilst the induced voltages are calculated by using the FDTD solution of the LEMP-to-line coupling model proposed by Agrawal *et al.* [6] included in the LIOV code [7]. For the case of a single conductor overhead lossless line, the model is represented by the following equations:

$$\frac{\partial v^s(x,t)}{\partial x} + L' \frac{\partial i(x,t)}{\partial t} = E_x^e(x,h,t) \quad (1)$$

$$\frac{\partial i(x,t)}{\partial x} + C' \frac{\partial v^s(x,t)}{\partial t} = 0 \quad (2)$$

$$v(x,t) = v^s(x,t) - \int_0^h E_z^e(x,z,t) dz \quad (3)$$

where: $v(x,t)$ is the total voltage along the x axis of the conductor and at time t ; v^s represents the so called scattered voltage and i the current; L' and C' are per unit length parameters of the line of height h ; E_x^e and E_z^e are two components of the lightning-originated exciting electric field (the horizontal electric field, namely the electric field component along the line direction, and the vertical component, respectively) calculated by using the FEM model that takes into account the presence of buildings nearby the line. In the LIOV code, the coupling model is numerically solved by applying a second order FDTD scheme [8], [9].

In [10] the application of a Monte Carlo procedure based on the accurate calculation of the induced voltages provided by the LIOV-EMTP-RV code for the evaluation of the lightning performance of an entire real distribution feeder has been presented. The implementation of a FEM model able to calculate the LEMP in a domain so large to contain a realistic power distribution network would require an excessive amount of computational resources. Therefore, this paper presents weighting functions that, applied to the electrostatic, induction and radiation field components calculated by using the *Master* and *Uman* equations [11], allow for a straightforward, accurate enough, calculation of the LEMP. The parameters of the weighting functions are identified by using the results obtained through the FEM model presented in [12], adapted in [5] to deal with the case of a single line shielded by nearby buildings.

The paper is structured as follows. Section II briefly reviews the FEM model for the LEMP calculation. Section III presents the weighting functions and the identification procedure of their parameters. Section IV shows the comparison between the induced voltages for different line configurations and presents a discussion of the results. Section V concludes the paper.

II. THE FEM MODEL

The considered cross-section geometries are shown in Fig. 1. A 1-km long 10-m high single-conductor overhead line

is placed parallel to one building (configurations A and B) or between two buildings (configurations C and D). The length of the buildings exceeds the line ends for 50 m, in order to study the relevant shielding effect for the whole length of the line. The cross-section width of each building is 10 m and the height is 15 m. The cross-section dimension has a minor influence on the LEMP attenuation, as verified by calculations.

Configuration B is motivated by the observation that the amplitude of the exciting electric field components that are responsible for the generation of lightning induced overvoltages is reduced also by buildings situated at the opposite side of the line with respect to the lightning channel [5]. Configurations C and D are considered as representative of urban overhead lines located at one of the sides of the roadway.

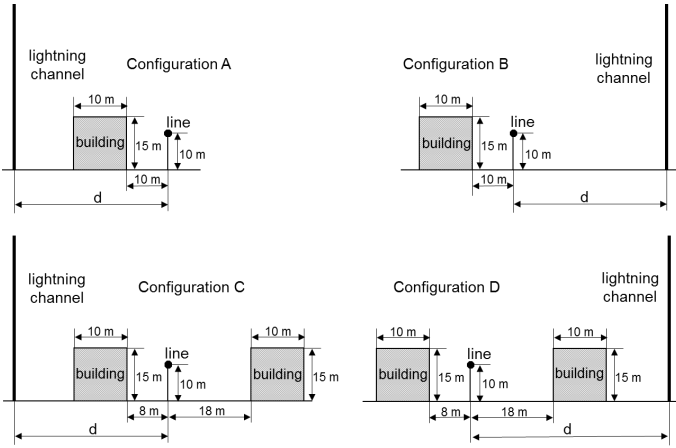


Figure 1. Considered line-building configurations: A and B with one building; C and D with the line in the space between two buildings.

The lightning channel, assumed as a straight vertical antenna 1.5 km high, is placed at distance d from the overhead line and equidistant to the line terminations.

The spatio-temporal distribution of the lightning current along the channel is defined by assuming the transmission line (TL) return stroke engineering model [13], with a return stroke wave-front velocity equal to 1.5×10^8 m/s and a current waveform represented by using the Heidler function [14]

$$i(0, t) = \frac{I_0}{\eta} \frac{(t/\tau_1)^n}{(t/\tau_1)^n + 1} \exp(-t/\tau_2) \quad (4)$$

$$\eta = \exp \left[\left(-\frac{\tau_1}{\tau_2} \right) \left(\frac{\tau_2 n}{\tau_1} \right)^{1/n} \right]$$

We have considered two different return stroke current waveforms, denoted in the following as waveform F and waveform S. Waveform F represents a first stroke by a single Heidler function with the following parameters: $I_0 = 29.3$ kA, $\tau_1 = 1.44$ μ s, $\tau_2 = 91.8$ μ s, $n = 2$. Waveform S represents a subsequent stroke by the sum of two Heidler functions with the following parameters: $I_{01} = 10.7$ kA, $\tau_{11} = 0.25$ μ s, $\tau_{21} = 2.5$ μ s, $n_1 = 2$, and $I_{02} = 6.5$ kA, $\tau_{12} = 2.1$ μ s, $\tau_{22} = 230$ μ s, $n_2 = 2$.

The 3D FEM model is used to calculate the LEMP in the absence of the line by means of the RF Module of the Comsol Multiphysics software, which implements a weak-form

representation of the time-domain wave equation of the magnetic vector potential.

The model includes a 3D domain large enough so as to avoid the effects of reflections at the boundaries. Such a domain is represented by a quarter of a 1.5 km radius sphere with the lightning channel as vertical axis (the same results are obtained by using the entire upper hemisphere domain but with a much larger computational time).

As a first approximation, the ground plane is lossless and the building is represented by a cuboid with perfectly conducting surfaces. The internal volume of the cuboid is excluded from the calculation domain.

III. WEIGHTING FUNCTIONS OF THE LEMP EQUATIONS

As mentioned in the Introduction, the evaluation of the induced voltages by means of the Agrawal *et al.* coupling model requires the evaluation of E_x^e and E_z^e of the LEMP along the line conductors.

We will assume that the influence of the presence of the nearby buildings could be taken into account by multiplying each term (induction, radiation and static fields) of E_x^e and E_z^e by a correction function f of the type

$$f(r) = k_1 r^{-3} + k_2 r^{-2} + k_3 r^{-1} + k_4 \quad (5)$$

where r is the distance between the observation point and the lightning channel and k_1, k_2, k_3 and k_4 are parameters identified for each configuration of Fig. 1 and for each term of E_x^e and E_z^e .

The electric field components due to the small dipole at the height z' become:

$$dE_z(r, z, t) = \frac{1}{4\pi\epsilon_0} \left[f_{z,i}(r) \frac{2(z-z')^2 - r^2}{cR^4} i(z', t - R/c) + \right. \\ \left. - f_{z,r}(r) \frac{r^2}{c^2 R^3} \frac{\partial i(z', t - R/c)}{\partial t} + \right. \\ \left. + f_{z,s}(r) \frac{2(z-z')^2 - r^2}{R^5} \int_0^t i(z', \tau - R/c) d\tau \right] dz' \quad (6)$$

$$dE_x(r, z, t) = \frac{\cos \vartheta}{4\pi\epsilon_0} \left[f_{x,i}(r) \frac{3r(z-z')}{cR^4} i(z', t - R/c) + \right. \\ \left. + f_{x,r}(r) \frac{r(z-z')}{c^2 R^3} \frac{\partial i(z', t - R/c)}{\partial t} + \right. \\ \left. + f_{x,s}(r) \frac{3r(z-z')}{R^5} \int_0^t i(z', \tau - R/c) d\tau \right] dz' \quad (7)$$

where c is the speed of light, ϑ is the angle between the line and the direction of the radial electric field, R is the distance of the electric dipole at height z' from the observation point:

$$R = \sqrt{r^2 + (z-z')^2} \quad (8)$$

The field components E_x^e and E_z^e at a specific point of the line are obtained by integrating (6) and (7) along the lightning channel (real and image).

The identification of each parameter in (5) is obtained by the least-square minimization of the differences between the field components calculated by the FEM method and the relevant results obtained from (6) and (7) all along the line.

Tables I to IV show the values of the parameters for each of the configurations of Figure 1 and for each field term, obtained for the case of a distance $d = 50$ m by using the return stroke current waveform S.

The value of 50 m has been chosen in order to represent the LEMP near the channel, where all components of the field – static, induction and radiation – have a significant weight. We do not take into account the effect of the building on the lightning incidence, namely its effect on the prospective stroke location. Indeed, this study aims to provide an indication of the induced voltage reduction expected for lightning in urban areas where lightning in principle can hit also other structures different from the buildings shown in Fig. 1, for instance elevated objects nearby the line.

In order to illustrate the agreement between the results provided by the FEM model and those obtained by using (5)-(7), Fig. 2 shows the comparison between the average value of

the vertical component of the electrical field (i.e., $\frac{1}{h} \int_0^h E_z^e dz$)¹

obtained by using the FEM model of Configuration A and by using (5)-(7) with the parameters of Table I provided by the least-square optimization (in the figure legend, the relevant curves are denoted as FEM and LSQ, respectively). Fig. 2a) shows the comparison for an observation point located at a line termination, whilst Fig. 2b) refers to the mid-point of the line. The figures also show the curve relevant to E_z^e calculated in absence of the buildings. Similar good agreement has been obtained for E_x^e and for the other configurations of Fig. 1.

Using the same weighting factor parameters of Table I, the results obtained by applying (5)-(7) for configuration A with $d = 300$ m and return stroke current waveform S are compared with the corresponding ones obtained by the FEM model in Fig. 3, whilst for the case of configuration A with $d = 50$ m Fig. 4 shows the comparison relevant to waveform F.

These results show that the parameters presented in Table I to Table IV, although obtained for $d = 50$ m and for return stroke waveform S, provide good results also for different values of d and a very different current waveform (namely, waveform F). Therefore we can conclude that the parameters of the weighting functions are rather independent of the lightning return stroke current waveform – which is in part expected due to the linear relation between currents and fields – and of the distance between the line and the stroke location, in the considered range, a computational result that is worth of further investigation for different building-line configurations and soil parameters.

¹ As shown in [5], in presence of buildings the vertical field changes by varying the height of the observation point with respect to the soil surface, whilst without buildings the value of the vertical electric field is quite constant for different values of the height.

TABLE I. WEIGHTING FUNCTION PARAMETERS FOR CONFIGURATION A, $d=50$ m, RETURN STROKE CURRENT WAVEFORM S.

function	Values of the coefficients			
	k_1	k_2	k_3	k_4
$f_{z,i}$	-8.702 10^3	252.2	-10.72	0.5809
$f_{z,r}$	4.109 10^3	-133.5	-15.98	0.5544
$f_{z,s}$	7.903 10^3	-339.9	-1.431	0.5421
$f_{x,i}$	14.50 10^3	-484.3	-11.10	0.5515
$f_{x,r}$	2.546 10^3	382.6	-31.75	0.5233
$f_{x,s}$	15.30 10^3	-550.2	-3.456	0.5307

TABLE II. WEIGHTING FUNCTION PARAMETERS FOR CONFIGURATION B, $d=50$ m, RETURN STROKE CURRENT WAVEFORM S.

function	Values of the coefficients			
	k_1	k_2	k_3	k_4
$f_{z,i}$	-15.29 10^3	686.9	-0.1481	0.5487
$f_{z,r}$	-15.29 10^3	669.9	-0.4927	0.5197
$f_{z,s}$	-15.29 10^3	724.0	-2.825	0.5475
$f_{x,i}$	-15.29 10^3	588.9	12.71	0.4905
$f_{x,r}$	-15.28 10^3	498.2	23.26	0.4217
$f_{x,s}$	-15.29 10^3	666.9	7.301	0.5072

TABLE III. WEIGHTING FUNCTION PARAMETERS FOR CONFIGURATION C, $d=50$ m, RETURN STROKE CURRENT WAVEFORM S.

function	Values of the coefficients			
	k_1	k_2	k_3	k_4
$f_{z,i}$	-15.30 10^3	512.8	-7.272	0.3413
$f_{z,r}$	-8.702 10^3	279.5	-10.45	0.3167
$f_{z,s}$	-3.108 10^3	87.89	-1.782	0.3165
$f_{x,i}$	21.08	-231.6	-0.1000	0.2941
$f_{x,r}$	-15.31 10^3	102.6	-6.308	0.2473
$f_{x,s}$	15.30 10^3	-710.8	7.539	0.2743

TABLE IV. WEIGHTING FUNCTION PARAMETERS FOR CONFIGURATION D, $d=50$ m, RETURN STROKE CURRENT WAVEFORM S.

function	Values of the coefficients			
	k_1	k_2	k_3	k_4
$f_{z,i}$	-15.30 10^3	607.9	-6.636	0.3366
$f_{z,r}$	-15.30 10^3	574.9	-13.55	0.3208
$f_{z,s}$	-5.104 10^3	234.2	-2.379	0.3146
$f_{x,i}$	-15.30 10^3	542.7	-5.482	0.3064
$f_{x,r}$	-15.30 10^3	486.9	-11.62	0.2575
$f_{x,s}$	-8.704 10^3	297.4	-0.3814	0.2932

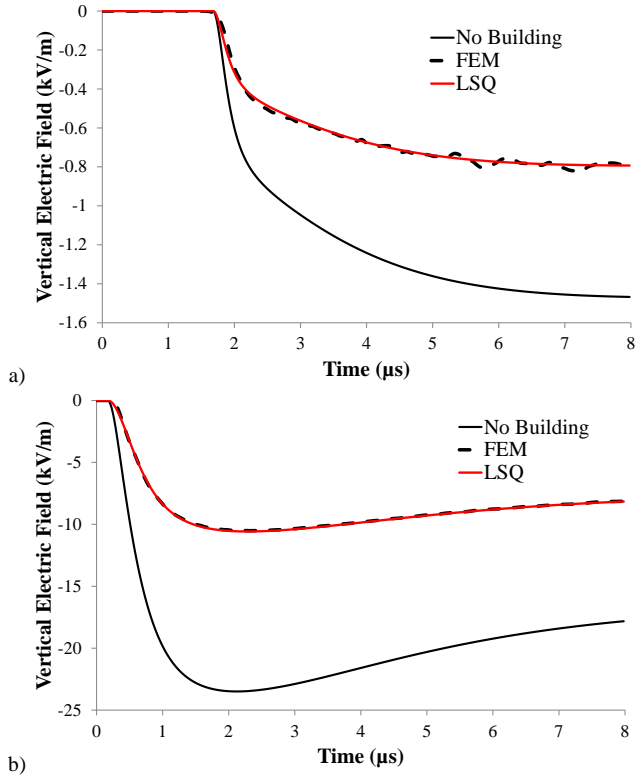


Figure 2. Average vertical electric field (configuration A, $d = 50$ m, waveform S): a) at the line terminations; b) at the mid-point of the line.

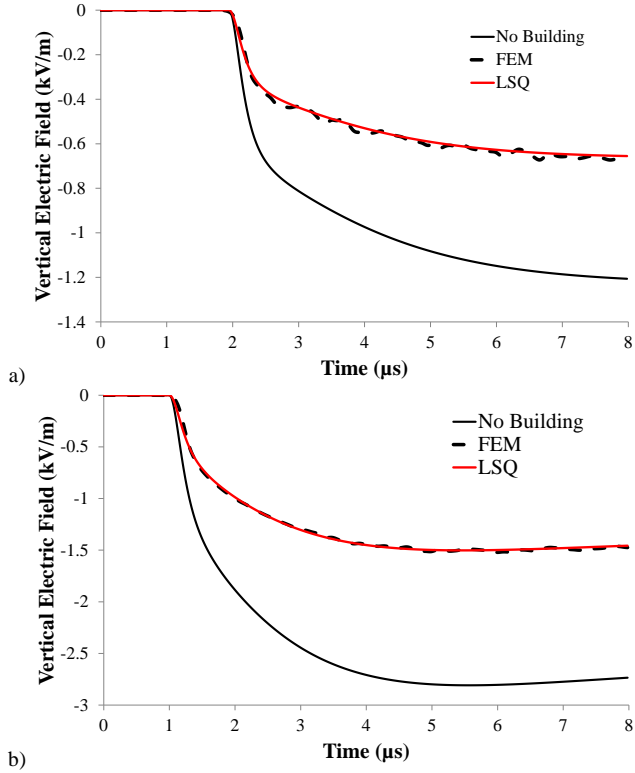


Figure 3. Average vertical electric field (configuration A, $d = 300$ m, waveform S): a) at the line terminations; b) at the mid-point of the line.

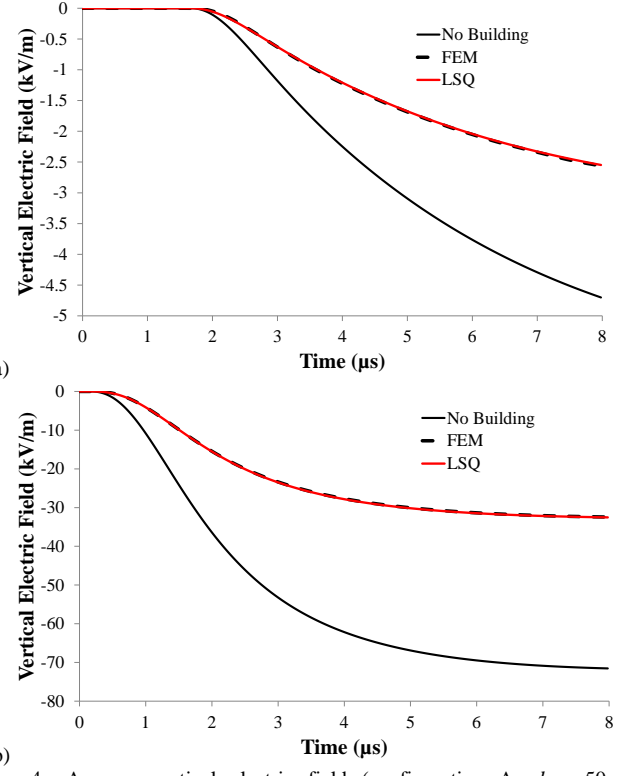


Figure 4. Average vertical electric field (configuration A, $d = 50$ m, waveform F): a) at the line terminations; b) at the mid-point of the line.

IV. INDUCED VOLTAGES IN PRESENCE OF NEARBY BUILDINGS

This section compares the induced voltages on the overhead line calculated by using the Agrawal *et al.* coupling model (1)-(3) implemented in the LIOV code for two differently-obtained exciting electric field components at each point of the line required by the FDTD solution method (a spatial step equal to 10 m is adopted in this paper):

- 1) E_x^e and E_z^e obtained by the FEM model;
- 2) E_x^e and E_z^e obtained by using equations (5)-(7) with parameters k provided by Table I – Table IV.

In the legends of the following figures, the results obtained by using 1) are denoted by FEM, whilst those obtained by using 2) are denoted by LSQ.

Figures 5 and 6 compare the induced voltages calculated by using 1) and 2) for all the four cases of Fig. 1. Moreover the figures show also the induced voltage calculated without the buildings.

For the case of configuration A, figures 7 and 8 compare the induced voltages calculated at the midpoint of the line for three different values of distance d , namely 50, 100, and 300 m. Fig. 7 refers to the case of return stroke current waveform S, whilst Fig. 8 refers to waveform F.

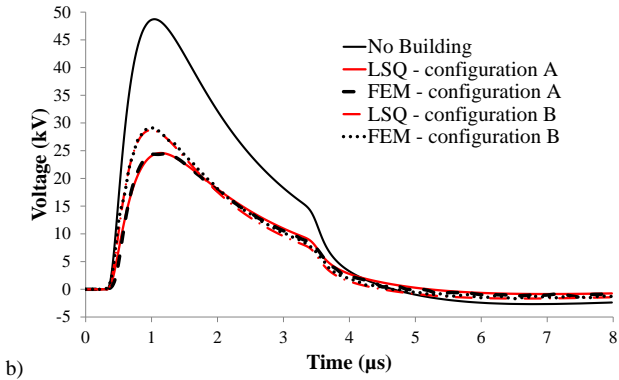
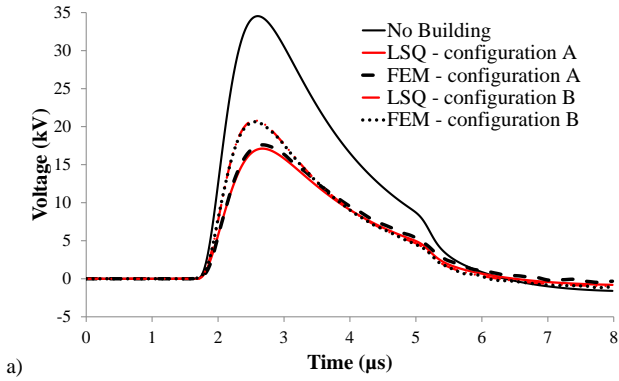


Figure 5. Induced voltages calculated for configuration A and configuration B for $d = 100$ m and waveform S: a) at the line terminations; b) at the mid-point of the line.

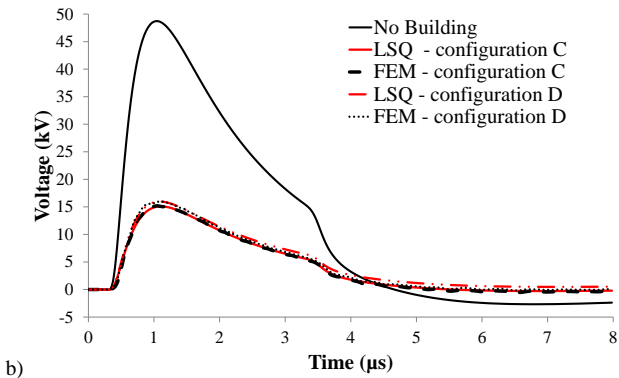
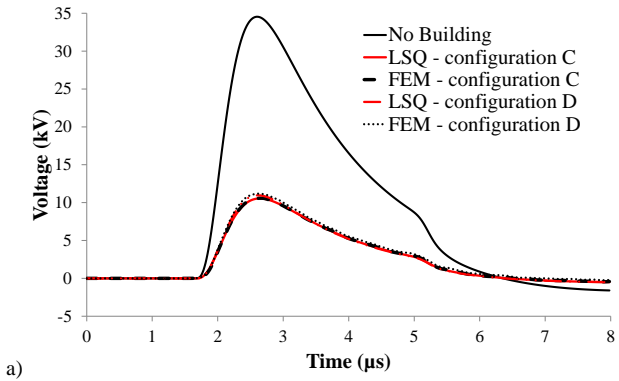


Figure 6. Induced voltages calculated for configuration C and configuration D for $d = 100$ m and waveform S: a) at the line terminations; b) at the mid-point of the line.

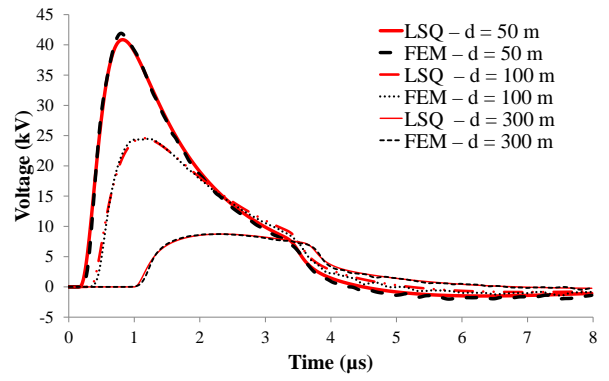


Figure 7. Induced voltages calculated for configuration A and waveform S at the mid-point of the line for three different values of d (50,100, and 300 m).

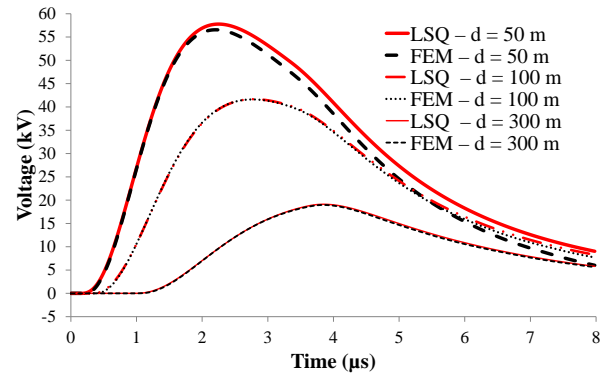


Figure 8. Induced voltages calculated for configuration A and waveform F at the mid-point of the line for three different values of d (50,100, and 300 m).

For all the considered cases, also for the induced voltages, a reasonable good agreement between the LSQ and FEM results has been obtained even for distances and return stroke current waveform different from those adopted for the identification of parameters k of Table I-Table IV.

The advantage of using equations (5)-(7) with respect to the use of the FEM model lies in the reduced computational effort. Whilst the induced voltage calculation by using (5)-(7) is performed in a few seconds for the case of a single line, the same calculation with the LEMP provided by the FEM model requires 5-6 hours.

As a final case, we consider a three-phase 2-km long 13.8 kV line. The conductors are placed 9.3 m above the ground in a horizontal configuration, with the central conductor at 150 cm and at 70 cm from the two lateral conductors. The line is matched at both terminations on its surge impedance matrix. In the line center, we assume the presence of an insulator with a withstand capability represented by the so-called disruptive effect (DE) model [15], [16]. The parameters of the implemented DE model are those provided in [17], assuming a critical flashover overvoltage (CFO) equal to 95 kV ($V_0 = 85.5$ kV, $k = 1$, $DE = 57.86$ kV $\cdot\mu$ s). The pole resistance (taken into account in the calculations when flashovers occur) is 400 Ω .

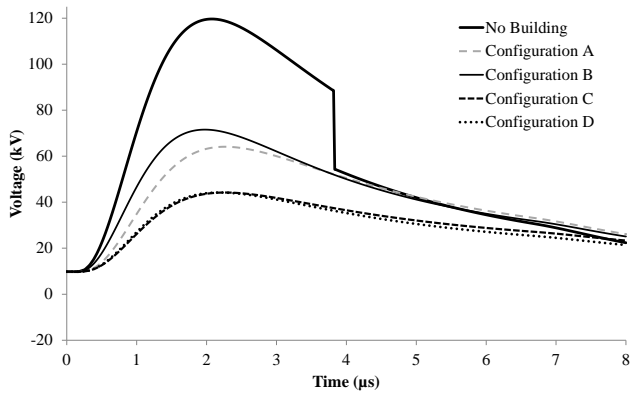


Figure 9. Comparison of the induced voltages at the mid-point of the line for $d=50$ m and return stroke current waveform F with and without buildings.

Fig. 9 shows the comparison between the induced voltages at the midpoint of the line, assuming the stroke location $d=50$ m far from the line and equidistant to the line terminations, for the case without buildings and for the four different configurations with buildings of Fig. 1. The adopted return stroke current is waveform F. At lightning occurrence, the voltages at the utility frequency of the three phase conductors are 9.8 kV, -9.8 kV, and 0 kV, respectively. Only the induced voltages relevant to the phase with the largest voltage value at the utility frequency are reported in Fig. 9.

The figure shows that only for the case without building, the insulator experiences a flashover. As in the previous cases the strongest reduction is achieved with buildings at both sides of the line. Fig. 9 appears to confirm the importance of the shield provided by nearby buildings in the evaluation of the lightning performance of overhead lines located in an urban area.

V. CONCLUSIONS

The results of this paper show that specific weighting functions can be introduced in the *Master* and *Uman* equations for the calculation of the electromagnetic field components due to a dipole at a specific height along the lightning channel in order to account for the effect of nearby buildings. The parameters of these weighting functions have been identified by using a FEM model for different configurations of an urban overhead line partially shielded by nearby buildings.

Such an approach reduces the burden typical of the use of 3D computationally intensive numerical models (based on, e.g., FDTD method or FEM).

The results show that the parameters are rather independent of the lightning return stroke current waveform and of the distance between the line and the stroke location, within the considered range.

For the configurations analyzed, the presence of the buildings may lead to a reduction ranging between one third to one half with respect to the case with no buildings.

Although this paper presents only results for the case of a single line, the method is conceived in order to be applicable for the lightning performance assessment of more topologically complex power distribution networks.

REFERENCES

- [1] A. Mosaddeghi, D. Pavanello, F. Rachidi, M. Rubinstein, and P. Zweigacker, "Effect of Nearby Buildings on Electromagnetic Fields from Lightning," *J. Light. Res.*, vol. 1, no. 1, pp. 52–60, 2009.
- [2] A. Piantini and J. M. Janiszewski, "Lightning induced voltages on distribution lines close to buildings," in *Proc. 25th Int. Conf. on Lightning Protection*, Rhodes, Greece, 2000.
- [3] A. Piantini, J. M. Janiszewski, A. Borghetti, C. A. Nucci, and M. Paolone, "A Scale Model for the Study of the LEMP Response of Complex Power Distribution Networks," *IEEE Trans. Power Deliv.*, vol. 22, no. 1, pp. 710–720, Jan. 2007.
- [4] T. H. Thang, Y. Baba, A. Piantini, and V. A. Rakov, "Lightning-Induced Voltages in the Presence of Nearby Buildings: FDTD Simulation Versus Small-Scale Experiment," *IEEE Trans. Electromagn. Compat.*, vol. 57, no. 6, pp. 1601–1607, Dec. 2015.
- [5] A. Borghetti, F. Napolitano, C. A. Nucci, and M. Paolone, "Effects of nearby buildings on lightning induced voltages on overhead power distribution lines," *Electr. Power Syst. Res.*, vol. 94, pp. 38–45, 2013.
- [6] A. K. Agrawal, H. J. Price, and S. H. Gurbaxani, "Transient Response of Multiconductor Transmission Lines Excited by a Nonuniform Electromagnetic Field," *IEEE Trans. Electromagn. Compat.*, vol. EMC-22, no. 2, pp. 119–129, May 1980.
- [7] C. A. Nucci and F. Rachidi, "Interaction of electromagnetic fields generated by lightning with overhead electrical networks," in *The Lightning Flash. 2nd Edition*, V. Cooray, Ed. IET - Power and Energy Series 69, 2014, pp. 559–610.
- [8] M. Paolone, C. A. Nucci, and F. Rachidi, "A new finite difference time domain scheme for the evaluation of lightning induced overvoltages on multiconductor overhead lines," in *Proc. 5th Int. Conf. on Power System Transients*, Rio de Janeiro, Brazil, 2001.
- [9] F. Napolitano, A. Borghetti, C. A. Nucci, M. Paolone, F. Rachidi, and J. Mahseredjian, "An advanced interface between the LIOV code and the EMTP-RV," in *Proc. 29th Int. Conf. on Lightning Protection*, Uppsala, Sweden, 2008.
- [10] F. Napolitano, F. Tossani, A. Borghetti, C. A. Nucci, M. L. B. Martinez, G. P. Lopes, G. J. G. Dos Santos, and D. R. Fagundes, "Lightning performance of a real distribution network with focus on transformer protection," *Electr. Power Syst. Res.*, 2016.
- [11] M. J. Master and M. A. Uman, "Electric and magnetic fields associated with establishing a finite electrostatic dipole: an exercise in the solution of Maxwell's equations," *Am. J. Phys.*, vol. 51, p. 118, 1983.
- [12] F. Napolitano, A. Borghetti, C. A. Nucci, F. Rachidi, and M. Paolone, "Use of the full-wave Finite Element Method for the numerical electromagnetic analysis of LEMP and its coupling to overhead lines," *Electr. Power Syst. Res.*, vol. 94, pp. 24–29, 2013.
- [13] M. A. Uman and D. K. Mclain, "Magnetic field of lightning return stroke," *J. Geophys. Res.*, vol. 74, no. 28, pp. 6899–6910, 1969.
- [14] F. Heidler, "Analytische blitzstromfunktion zur LEMP-berechnung," in *Proc. 18th Int. Conf. Lightning Protection*, Munich, Germany, 1985.
- [15] R. L. Witzke and T. J. Bliss, "Surge Protection of Cable-Connected Equipment," *Trans. Am. Inst. Electr. Eng.*, vol. 69, no. 1, pp. 527–542, 1950.
- [16] R. Caldwell and M. Darveniza, "Experimental and analytical studies of the effect of non-standard waveshapes on the impulse strength of external insulation," *IEEE Trans. Power Appar. Syst.*, vol. PAS-92, no. 4, pp. 1420–1428, Jul. 1973.
- [17] A. De Conti, E. Perez, E. Soto, F. H. Silveira, S. S. Visacro, and H. Torres, "Calculation of Lightning-Induced Voltages on Overhead Distribution Lines Including Insulation Breakdown," *IEEE Trans. Power Deliv.*, vol. 25, no. 4, pp. 3078–3084, Oct. 2010.